Applied Thermal Engineering 72 (2014) 62–69

Contents lists available at ScienceDirect

Applied Thermal Engineering

journal homepage: www.elsevier.com/locate/apthermeng

A numerical study on the theoretical accuracy of film thermal conductivity using transient plane source method

Hu Zhang, Ming-Jia Li, Wen-Zhen Fang, Dan Dan, Zeng-Yao Li, Wen-Quan Tao*

Key Laboratory of Thermal Fluid Science and Engineering of MOE, School of Energy and Power Engineering, Xi'an Jiaotong University, Xi'an, Shaanxi 710049, China

HIGHLIGHTS

- Numerical method is used to analyze the test accuracy of film thermal conductivity.
- The theoretical assumptions of transient plane source method are verified.
- The accuracy of transient plane source method varies with thermal resistance of film.
- The accuracy of film conductivity measurement could be improved via modification.

GRAPHICAL ABSTRACT

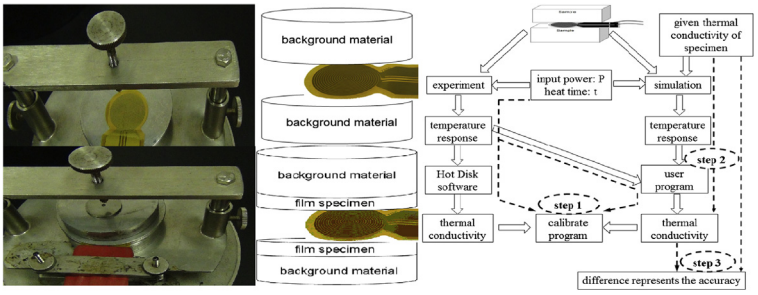

ARTICLE INFO

Article history:
Received 29 September 2013
Accepted 25 January 2014
Available online 3 February 2014

Keywords:
Numerical study
Thermal conductivity accuracy
Film specimen
Transient plane source method

ABSTRACT

The thermal conductivity of film specimen is different with bulk materials and lack of standard reference materials, and few study of the measurement accuracy of film thermal conductivity has been reported. A numerical study is conducted to analyze the theoretical accuracy of film thermal conductivity introduced by the assumption of transient plane source method. In the data reduction from the measurement results, it is difficult to determine the calculation area and thickness due to the non-ideal 1D heat conduction generated in the film and the heat element has a certain thickness. The simulation found that if the thermal resistance of the film to be measured is comparable or higher than that of the sensor insulation layer, the accuracy of determining the film thermal conductivity would be very high. The theoretical accuracy of transient plane source method can be as small as ±6% after some modification.

1. Introduction

Film specimens are widely used in measurements of electronics, mechanics, chemicals and other industries. The thermal conductivity is a key property of film specimens, such as proton exchange membrane and gas diffusion layer in fuel cell [1–7]. Many steady methods and transient methods are developed to measure the thermal conductivity of micro/nano films, such as one dimensional steady state method, 3ω method, hot wire/strip method, laser flash method, transient plane source (TPS) method, photoacoustic method, optothermal method and micro-Raman spectroscopy method [8–18]. The thermal conductivity of film specimen may differ greatly from bulk specimen because of the phonon scattering at surfaces and different manufacturing process [9]. In addition, thin thickness of film and lack of standard reference sample make it difficult to measure film thermal conductivity accurately. Often different method may have different result for the same film specimen [12].

TPS method is adopted widely to measure thermal conductivity of bulk specimens [19,20]. The method has been extended to measure thermal conductivity of anisotropic bulk specimens, slab

* Corresponding author. Tel./fax: +86 (0)29 82669106.
E-mail addresses: huzhang522@stu.xjtu.edu.cn (H. Zhang), mjli0703@stu.xjtu.edu.cn (M.-J. Li), fangwenzhen@126.com (W.-Z. Fang), dan.wishes@stu.xjtu.edu.cn (D. Dan), lizengy@mail.xjtu.edu.cn (Z.-Y. Li), wqtao@mail.xjtu.edu.cn (W.-Q. Tao).

1359-4311/$ – see front matter © 2014 Elsevier Ltd. All rights reserved.
http://dx.doi.org/10.1016/j.applthermaleng.2014.01.058

specimens and thin film specimens [12,19,20]. This method can measure film specimen with thickness ranging from 10 μm to 1 mm according the ISO standard [12,13,21]. However, to the authors' knowledge the accuracy of TPS method of measuring film specimen has not been discussed in the open literature. The source of measurement uncertainty of dynamic test can be divided into two aspects [22]. The first part represents the deviation of the mathematical assumption of the method from the practical measurement and the second part represents the deviation caused by the input parameter of measurement and evaluation procedure. For TPS method, many works of parameter estimation have been conducted to analyze the temperature measurement uncertainty using least-squares procedure and the data evaluation method to improve the accuracy [22–26]. The uncertainty of measuring voltage, resistance, diameter, thickness, temperature coefficient of the resistivity of the sensor, etc, has been discussed by Suleiman and Malinarič [24]. However, few works consider the deviation caused by the theoretical assumption. In our previous works [27–29], the influence of insulating layer of the Hot Disk sensor on the bulk specimen thermal conductivity measuring accuracy was analyzed through numerical simulation. The simulation considered the actual thickness of the test sensor instead of treating the sensor as plane source without thickness and neglecting the heat loss through the sensor side. Previous simulation by TPS method in literature [19] was also conducted to analyze the accuracy of hot-disk technique when applied to low-density insulating materials. In this paper, the theoretical analysis for the thermal conductivity measurement accuracy of thin film specimens using TPS method is conducted through numerical simulation, seemingly first in the literature. Film specimens with different thickness and thermal conductivity are numerically studied. The simulation results will reveal the theoretical accuracy of TPS method introduced by the model assumption on measuring film specimens.

The outline of the rest of the paper is as follows. The test theory of TPS method will be briefly introduced firstly for the reader's convenience. Then the numerical method adopted in this work is presented, followed by the numerical results and discussion. Finally some useful conclusions are summarized.

2. Theoretical basis of TPS method

TPS method is proposed by Gustafsson [30] to measure thermal conductivity of bulk specimens, thin slab specimens and film specimens. TPS method became an ISO standard for determining thermal conductivity and thermal diffusivity of plastics [13] in 2008. Fig. 1(a) shows the kapton7280 sensor used to measure thermal conductivity of the film specimens. The sensor consists of a double spiral heating element and two thin insulation films packed on both sides of the spiral structure to keep the shape and electric insulation. The heating element is usually made of nickel and the insulation film is made of kapton.

The double spiral sensor is used both as a heat source and as a dynamic temperature sensor. When the sensor is electrically heated, the electric resistance increases as a function of time and can be given by the following expression:

$$R(t) = R_0(1 + \alpha\Delta T) = R_0[1 + \alpha\Delta T_i + \alpha\Delta T(\tau)] \quad (1)$$

where t is the test time, s; R_0 is the resistance of sensor at time $t = 0$, Ω; τ is the dimensionless time defined as $\tau = \sqrt{t/\Theta}$, here Θ is the characteristic time defined by $\Theta = r^2/a$, r is the radius of sensor, mm, a is the thermal diffusivity of background material, $mm^2\ s^{-1}$; α is the temperature coefficient of the resistivity, 1/K; ΔT

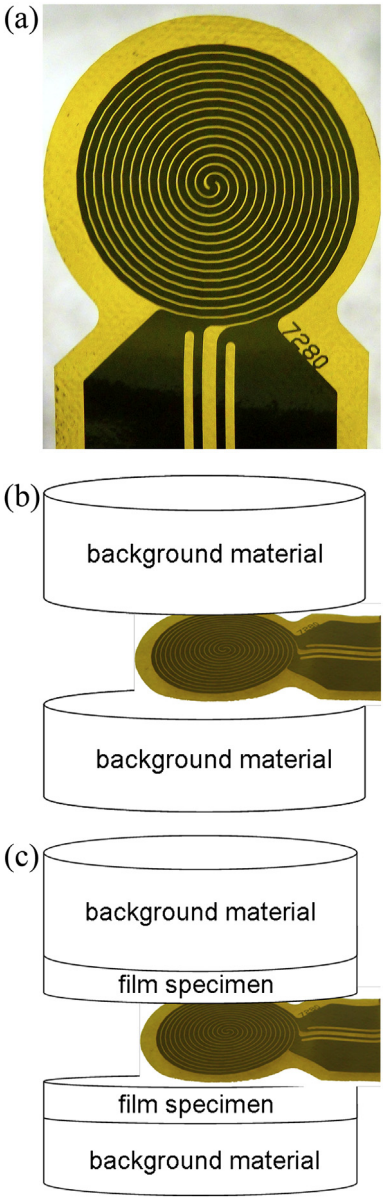

Fig. 1. Sensor profile and schematic of experiment (a) kapton7280, (b) kapton insulation layer and (c) film specimen.

is the mean temperature increase of the probe; ΔT_i is the temperature difference across the film, K; $\Delta T(\tau)$ is the temperature increase of the background material surface facing the sensor, K. The value of ΔT_i will becomes constant after a short time provided that the insulation film is thin and the power output is constant. With the assumption that the bifilar probe can be simplified with a number of concentric and equally spaced circular line sources, the solution of the thermal conductivity equation is given by [13,31]

$$\Delta T(\tau) = \frac{P_0}{\pi^{3/2} r\lambda} E(\tau) \quad (2)$$

where, P_0 is the power output of the sensor, W; λ is the thermal conductivity of the test sample, $W\ m^{-1}\ K^{-1}$. When determining the thermal conductivity of film specimen, λ is the thermal conductivity of the background material. $E(\tau)$ is the dimensionless time function, defined as

$$E(\tau) = [m(m+1)]^{-2}\int_0^{\tau}\sigma^{-2}\left[\sum_{l=1}^{m} l\sum_{k=1}^{m} k\times\exp\left(\frac{-(l^2+k^2)}{4m^2\sigma^2}\right)I_0\left(\frac{lk}{2m^2\sigma^2}\right)\right]\left[1+2\sum_{i=1}^{\infty}\exp\left(-\frac{i^2}{\sigma^2}\frac{h^2}{r^2}\right)\right]d\sigma \quad (3)$$

where I_0 is the modified Bessel function; m is the number of concentric ring sources, h is the thickness of the slab. The detailed derivation was presented in [31].

Substituting Eq. (2) into Eq. (1) and denoting $R^* = R_0(1+\alpha\Delta T_i)$, $C = \alpha R_0 P_0/\pi^{3/2} r\lambda$, Eq. (1) can be rewritten as

$$R(t) = R^* + CE(\tau) \quad (4)$$

ΔT_i becomes constant after a short time [28,29] and it will also be proved in this work. Hence R^* has the same variation trend as ΔT_i. C is a constant for an established measurement system. As shown in Eq. (4), $R(t)$ increases linearly with $E(\tau)$. When measuring thermal conductivity of bulk specimens or slab specimens, input power and heating time are given. The temperature of the source increases when the probe begins to heat. The thermal resistance of the probe changes with the temperature. The temperature increase of the source is obtained by measuring the voltage imbalance and the current according to the test electrical bridge shown in the ISO22007-2 standard. The temperature coefficient of resistance of the heat element is available. Then the temperature increase curve with time of the probe can be obtained. Finally the linear relationship shown in Eq. (4) is established by a least-squares fitting procedure with the constraint condition of best linearity. Then the thermal diffusivity of the background material is obtained from the final step of the iteration procedure and the thermal conductivity of the background material is determined from the slop of the line. The intercept of the fitting line of the temperature increase curve is temperature difference across the film, ΔT_i. The thermal conductivity of film specimen can be calculated by

$$\lambda_i = P_0\delta/(2A\Delta T_i) \quad (5)$$

where δ is the thickness of the film and A is the area of the probe.

According to ISO22007-2 when performing thermal conductivity measurement of film specimen, two dynamic tests should be conducted [13]. The first measurement is conducted with the sensor placed between two plane high thermal conductivity materials as shown in Fig. 1(b). The thermal conductivity of insulation layer of the sensor together with the adhesive (used to attach the insulation layer and the heat source), $\lambda_{\text{insulation}}$, can be determined in this measurement. The second measurement is conducted with the two thin film specimens placed between the sensor and the slab high thermal conductivity materials as shown in Fig. 1(c) to obtain the effective thermal conductivity of the insulation layer and the thin film specimen, λ_{total}. From Eq. (6)

$$\frac{\delta_{\text{insulation}}+\delta_{\text{specimen}}}{\lambda_{\text{total}}} = \frac{\delta_{\text{insulation}}}{\lambda_{\text{insulation}}} + \frac{\delta_{\text{specimen}}}{\lambda_{\text{specimen}}} \quad (6)$$

the thermal conductivity of the film specimen, $\lambda_{\text{specimen}}$ can be calculated, where $\delta_{\text{insulation}}$ and δ_{specimen} are the thickness of the insulation layer and the thin film specimen, respectively.

3. Numerical simulation method

3.1. Flow chart of the simulation

The exact thermal conductivity of the film is unavailable. As described in Section 2, the theory of determining the thermal conductivity of film is quite complicated. Therefore, the error or uncertainty introduced by the theoretical assumption could not be easily obtained and this makes it difficult to analyze the measurement accuracy. However, the theoretical accuracy of film thermal conductivity measured by TPS method can be determined through simulation as follows. In the simulation, the heat transfer process of the experimental measurement is numerically simulated by mimicking the process on which the TPS measurement theory is based. The geometry parameters, heating power and heating time are the same with that in the experiment test. The thermal conductivity of the film to be determined in the simulation is given beforehand. The temperature of the heat source is monitored in the simulation and then the thermal conductivity of the film can be calculated according to the TPS theory. If the calculated film thermal conductivity is identical with the given value, there has no error brought by the theoretical assumption of TPS. Otherwise, the difference between the given value and the calculated value obtained from the simulation represents the theoretical measurement error of TPS method. This simulation procedure of determining the theoretical accuracy is illustrated in Fig. 2. They are described below in details.

Firstly, a program should be developed to calculate the thermal conductivity of the film specimens once the temperature response of the sensor through simulation is obtained. The software embedded in Hot Disk could be used to calculate the film thermal conductivity from the temperature response of sensor that was measured in the experiment. But it could not be used to calculate the thermal conductivity from the temperature response of sensor that monitored in the simulation because the Hot Disk software is a black box to the users. Therefore, a self-developed program is needed to calculate the thermal conductivity from simulated sensor temperature response. The self-developed program could be verified with the Hot Disk software by calculating the same temperature increase curve of the sensor. If the results calculated by self-developed program is identical to that obtained from the

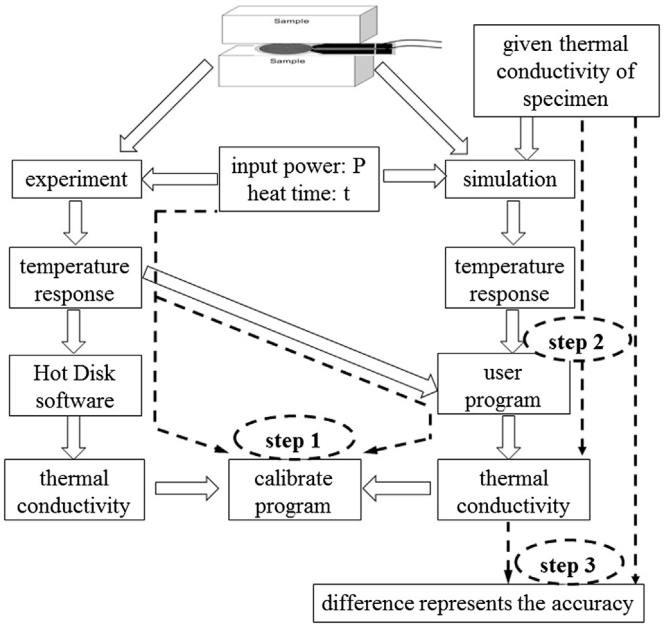

Fig. 2. Flow chart of the simulation.

instrument software, the self-developed program could be used to determine the film thermal conductivity from the temperature response of the sensor in the simulation.

Secondly, the dynamic heat transfer process of the thermal conductivity measurement of film specimen is simulated by FLUENT software. In the simulation, the geometry parameters, heating time power and heating are in accordance with that in practical test. The thermal conductivity of film specimen is given in the simulation. The temperature response of the sensor is monitored in the simulation and then the thermal conductivity of the film specimen could be calculated by the self-developed program.

Finally, the calculated thermal conductivity is compared with the given value before simulation. The difference between the calculated value and the given value represents the uncertainty brought in by the theoretical assumptions of TPS theory. The simulation is conducted with different film thermal conductivity and different film thickness to reveal their effects on the theoretical accuracy.

3.2. Computational domain

The dynamic test process can be regarded as an unsteady heat conduction problem consisted of a series of concentric heating elements in a finite space. According to the axis-symmetrical geometry, the 3D heat conduction problem can be simplified into 2D one with one radian being adopted as the representative for the circumferential direction. A schematic diagram of the computational domain is shown in Fig. 3.

In the domain, zone 1 is the heat source (nickel), zone 2 is the insulation layer (kapton), zone 3 is the background material (stainless steel) to fix the film specimen and zone 4 is the test film specimen. The detail geometry of the simulation is presented in Table 1. Table 2 shows the thermal property used in the simulation. All simulations are conducted with heating power 1 W, iterative time step 0.01 s, and total simulation time 10 s.

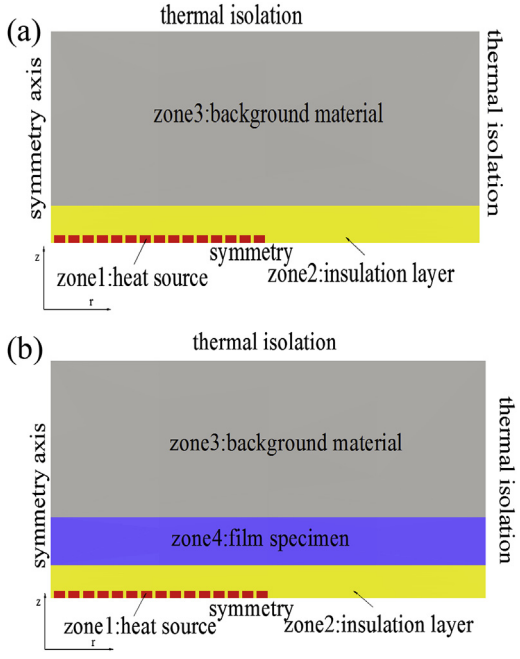

Fig. 3. Schematic diagram of the computational domain (a) insulation film and (b) insulation film and film specimen.

Table 1
Simulation condition.

Parameter	Size
Thickness/width of nickel	4 μm/0.8 mm
Interval between nickel	0.2 mm
Number of concentric ring	15
Thickness of kapton	28 μm
Thickness of stainless steel	1.95 mm
Radius of background materials/film specimen	30 mm
Film specimen thickness	25/50/100/200 μm

3.3. Governing equation and boundary conditions

The governing equation of the 2D axis-symmetrical cylindrical non-steady state heat conduction with internal heat source is shown as follows [32]:

$$\rho c\frac{\partial T}{\partial \tau}=\frac{1}{r}\frac{\partial}{\partial r}\left(\lambda r\frac{\partial T}{\partial r}\right)+\frac{\partial}{\partial z}\left(\lambda\frac{\partial T}{\partial z}\right)+\dot{\Phi} \tag{7}$$

The boundary conditions of the problem are as follows:

Left side: axis symmetry.
Downside: symmetry.

Outside of the background materials (top side and right side): thermal isolation. Because the thermal conductivity of background material (13.7 W m^{-1} K^{-1}) is as high as more than 500 times of the surrounding air (0.026 W m^{-1} K^{-1}), the top and right walls can be treated as adiabatic with enough accuracy.

Heat source: given volumetric intensity of power input.
Interfacial boundary: interior. It is a default boundary condition in FLUENT software. The continuity of temperature and heat flow on the interfacial boundary will be satisfied automatically under the interior condition.

3.4. Numerical methods

The simulation is conducted by commercial software FLUENT 6.3.26. The grid size is non-uniform because the geometry size of the heat source (μm), the insulating layer (μm), the film specimen (μm) and the background material (mm) in the computational domain has different order of magnitude. The grid numbers of the six cases with film specimens thickness of 0 μm (to determine the thermal conductivity of kapton insulation layer), 25 μm, 50 μm, 100 μm, 200 μm and 500 μm are 1,083,000, 1,390,000, 1,358,400, 1,308,000, 1,698,000 and 1,602,000 respectively, with the cross section of each micro heating element can be distinguished individually. These grid numbers are obtained after the grid-independent examination. The 1st-order implicit formulation is adopted to solve the 2D unsteady state heat conduction problem, and the diffusion term is discretized by the central difference. The heat sources are treated as discrete heat sources with a finite volume. The temperature of the heat sources and the temperature of

Table 2
Thermal property.

Material	λ/W m^{-1} K^{-1}	ρ/kg m^{-3}	c_p/J kg^{-1} K^{-1}
Nickel	91.4	8900	444
Stainless steel	13.7	8000	460
Kapton	0.033	1000	500
Film specimen	0.033/0.06/0.1/0.2/0.5/1	1000	500

the background material surface that facing film specimen are non-uniform. Therefore, the temperature of heat sources is obtained by volume average and the temperature of sample surface facing film is determined by area weighted average.

4. Results and discussion

4.1. The validation of thermal conductivity determination program of the film specimen

As indicated above the software supplied by the instrument is a black box and inherently connected with measurement steps, it cannot be used to calculate the temperature increase curve of the heating source obtained through simulation. Therefore, an independent program is developed to calculate the thermal conductivity from the temperature increase curve of the sensor obtained by numerical simulation. The self-developed program for determining thermal conductivity of film specimens is validated by comparing with Hot Disk Thermal Constants Analyzer by calculating the same temperature response of sensor measured in the experiment. The test parameters of the experiment are as follows:

Thickness of kapton insulation layer: 25 μm.
Thickness of Poly Ethylene (PE) film: 100 μm.
Thickness of gas diffusion layer (GDL): 590 μm.
Thickness/radius of background material (stainless steel): 1.95 mm/30 mm.
Heating power: 1 W.
Measurement time: 20 s.
Radius of sensor: 14.67 mm.
Sensor area: 727 mm^2.

Fig. 4(a) shows the temperature increases of source when measuring kapton insulation layer and PE film. Fig. 4(b) shows the regressed results of the linear relationship between temperature increase and the dimensionless time function $E(\tau)$. It can be seen from the figure that the slope and intercept of the line calculated from the Hot Disk software and from the self-developed program are close to each other. The thermal conductivity of film specimen obtained from the instrument software and the self-program is shown in Table 3. The thermal conductivities of the kapton insulation layer, PE film and GDL calculated from the self-program show good agreement with that calculated from the embedded software with the maximum deviation less than ±1%. The comparison proves that the self-developed program could calculate the thermal conductivity of film accurately once obtained the temperature increase of sensor.

4.2. Problems of determining film thermal conductivity

The sensor area (kapton7280: 727 mm^2 including the area of the kapton insulation filled among the adjacent rings) and the insulation thickness (25 μm) in the calculation is the same as the instrument software. However, the heat element has a double spiral structure (in black color) with width of 0.8 mm and the kapton insulation (in yellow color in the web version) with width of 0.2 mm is filled among the adjacent rings as shown in Fig. 1(a). The actual heating area is not 727 mm^2. Therefore, whether the calculation area in Eq. (5) should include the insulation part among the adjacent rings or not needs to be reconsidered. In addition, the film thermal conductivity is sensitive with the calculation thickness of the sensor described in Eq. (5). In the Hot Disk software, δ_i including the thickness of heat source is selected for calculation. It is worth noting that the selection of calculation thickness is another issue because the heating element of the sensor has a certain thickness

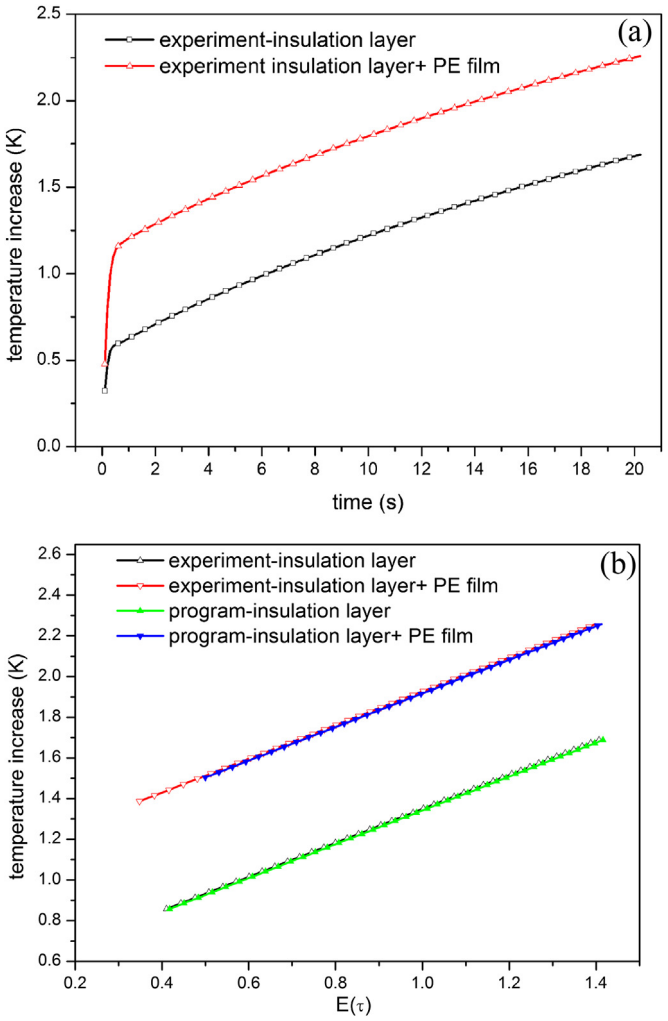

Fig. 4. Temperature increases of source: (a) temperature increase curve and (b) calculated linear relationship.

and gaps between two adjacent heating rings are filled with kapton insulation.

4.3. The accuracy of determining the thermal conductivity of kapton insulation layer

The simulation is firstly conducted to determine the thermal conductivity of the sensor insulation layer as shown in Fig. 3(a). The temperature increase curves versus time of the heat source and the sensor surface are monitored. The difference between them represents the thermal resistance of the kapton insulation layer (Fig. 5). As shown in the figure, the temperature difference across the sensor insulation layer will become constant after 0.25 s and remains constant throughout the simulation.

Table 3
Validation of the program.

λ/W m^{-1} K^{-1}	Measured by Hot Disk	Calculated by program	Deviation/%	Test information
Kapton layer	0.0333	0.0336	0.90	25 μm/24 °C
	0.0611	0.0606	−0.82	25 μm/90 °C
PE film	0.1198	0.1205	0.58	100 μm
GDL	0.2593	0.2594	0.04	590 μm

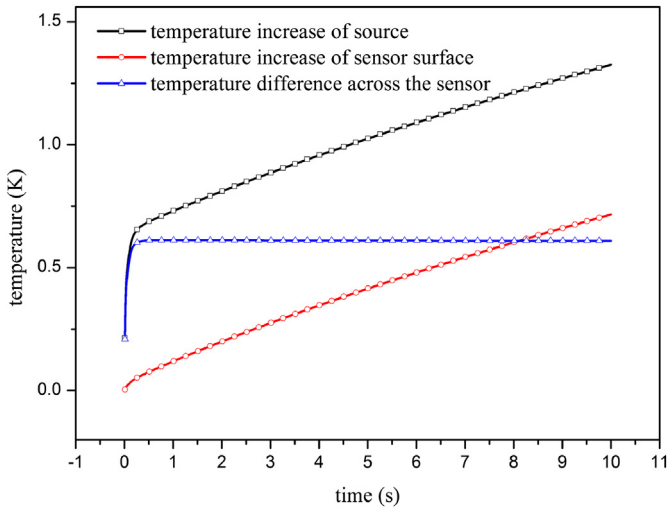

Fig. 5. Temperature increase curve of source, sensor surface and difference.

The thermal conductivity and thermal diffusivity of the background material (stainless steel) given in the simulation are 13.7 W m^{-1} K^{-1} and 3.72 mm^2 s^{-1}, respectively. The calculated properties of stainless steel from the temperature increase curve of the heat source are 13.96 W m^{-1} K^{-1} and 3.79 mm^2 s^{-1}, respectively, with a deviation of 1.9%. It proves that the TPS method can measure the slab material with high thermal conductivity accurately. Table 4 shows the calculated thermal conductivity of kapton insulation layer with given value of 0.033 W m^{-1} K^{-1}. In the simulation, the radius of the outmost ring is 15 mm and the total area of the heat element and the gap in the simulation is 707 mm^2. The actual heating area in the simulation is 573 mm^2. Different calculation thickness is selected to compare their accuracy. The calculation thickness is 28 μm (δ_1) when taking account of the thickness of the heat element. When excluding the thickness of the heat element, the calculation thickness is 24 μm (δ_2). The calculation thickness of their median is 26 μm. For constant calculation area, the thermal conductivity of insulation layer is proportional to its thickness as shown in Eq. (5). When take the actual heating area to calculate, the thermal conductivity of kapton insulation is overestimated while it is underestimated when choosing the total sensor area. For the kapton insulation layer, both the actual heat area and total sensor area are optional with deviation within ±3% when choosing δ_2 and δ_1 as the calculation thickness respectively.

4.4. The accuracy of determining the thermal conductivity of film specimens

In this section, the test accuracy of film specimens with thickness of 25 μm, 50 μm, 100 μm, 200 μm, 500 μm are simulated for TPS method. The schematic diagram of the simulation is shown in Fig. 3(b). The simulated thermal conductivity range of film specimen with certain thickness is from 0.033 W m^{-1} K^{-1} to 1 W m^{-1} K^{-1}. The simulated theoretical accuracy of film specimens with different thickness and thermal conductivity are shown in Fig. 6. When selecting the actual heating area and the insulation thickness excluding heat element for thermal conductivity determination, it will be overestimated. The deviation increases with thermal conductivity and the deviation is extremely high when measuring thin materials with high thermal conductivity. On the contrary, when selecting the total sensor area and the insulation thickness including heat element, the thermal conductivity is underestimated. However, the deviation

Table 4
Influence of area and thickness.

λ/W m^{-1} K^{-1}	$\delta_1 = 28$ μm	$(\delta_1 + \delta_2)/2 = 26$ μm	$\delta_2 = 24$ μm
$A = 573$ mm^2	0.0396	0.0368	0.034
Deviation/%	20.0	11.2	3.0
$A = 707$ mm^2	0.0321	0.0298	0.0275
Deviation/%	−2.7	−9.7	−16.7

obtained by this way is much better than the former one and it is the choice of instrument software. The deviation increases with thermal conductivity and the deviation is also very large when measuring thin materials.

Dozens percent of deviation is not acceptable for film thermal conductivity measurement. So it motivates more studies about where the deviation comes from and whether it could be improved. The determination of film thermal conductivity in Eq. (5) is based on 1D heat conduction assumption. Kapton insulation is filled between the heat elements to keep electric insulation. Therefore, the heat generates from the heat element will transfer to the entire region, which is not an ideal 1D heat transfer process. So the deviation is caused by the theoretical assumption deviates from the practical measurement condition.

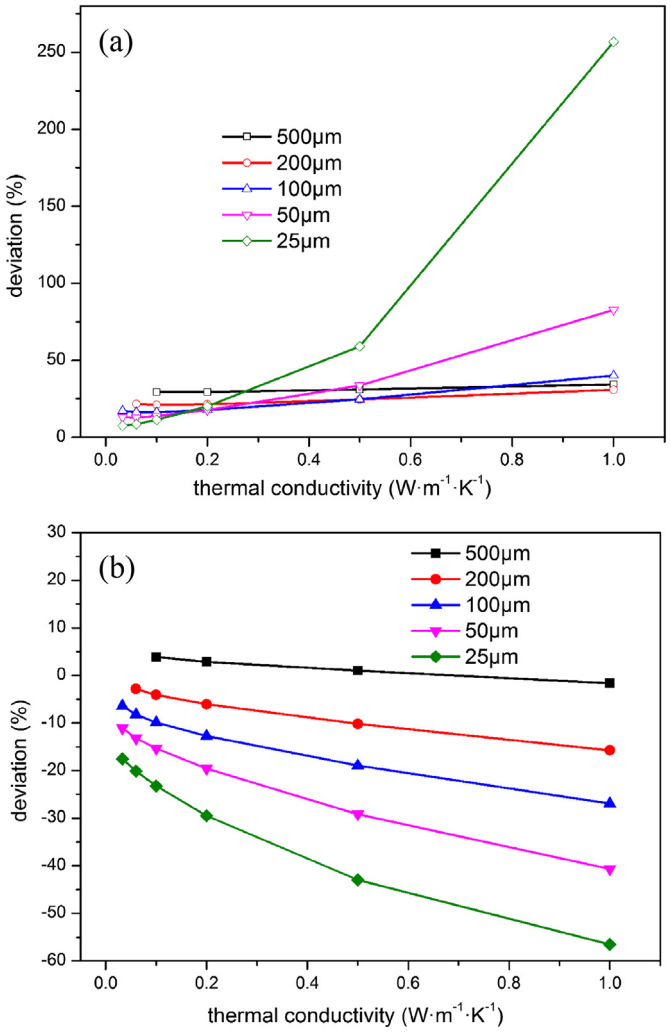

Fig. 6. Deviation of film thermal conductivity (a) $A = 573$ mm^2, $\delta_{kapton} = 24$ μm and (b) $A = 707$ mm^2, $\delta_{kapton} = 28$ μm.

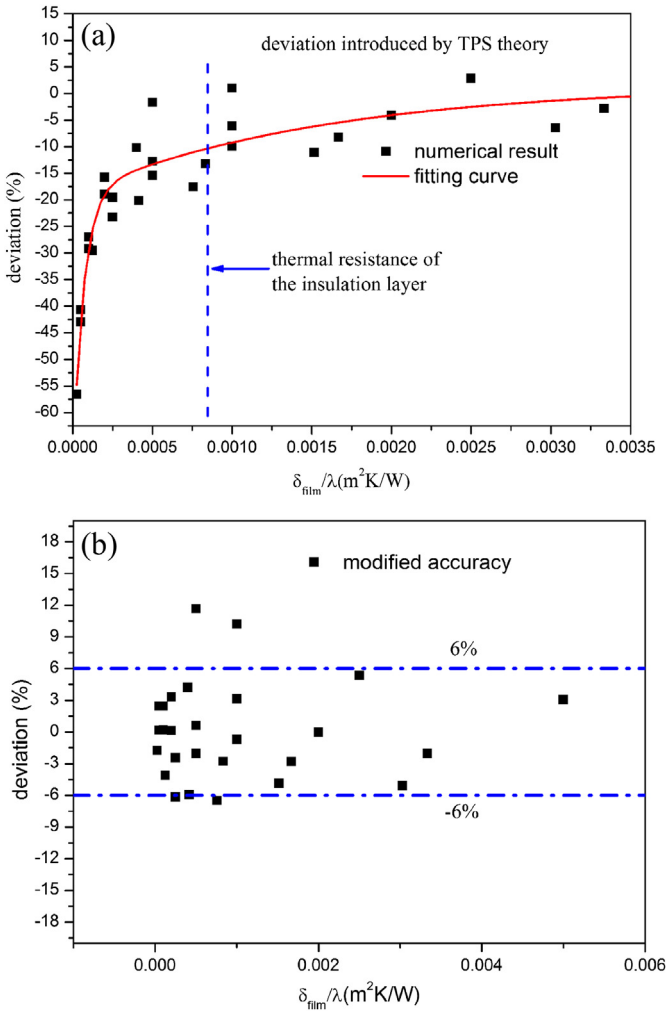

Fig. 7. Deviation versus thermal resistance of test film (a) before modified and (b) after modified.

As shown in Fig. 6(b), the deviation of film thermal conductivity decreases with the decrement of thermal conductivity or increment of film thickness. In other words, the higher the thermal resistance (δ/λ) of test film, the smaller the deviation. The deviation versus thermal resistance of film specimen taking the total sensor area for thermal conductivity determination is plotted in Fig. 7(a). The result clearly shows that the larger the thermal resistance, the less the deviation. In the simulation, the thermal resistance of the kapton insulation, $\delta_{insulation}/\lambda_{insulation}$, is 8.485×10^{-4} m^2 K/W. When the thermal resistance of test film is comparable or higher than that of the insulation layer, the deviation becomes acceptable. Because for this case the error brought in by non-ideal 1D heat conduction assumption of determining the thermal resistance of insulation layer has less influence on the thermal resistance of the test film as described in Eq. (6). The deviation versus thermal resistance of film specimen could be fitted by an exponential decay curve with a form as follows:

$$y = 1.69843 - 52.71338\exp(-x/0.000066533) - 20.59207\exp(-x/0.00157) \quad (8)$$

here, y is the deviation of thermal conductivity of film (%) and x is the thermal resistance of test film.

Then the deviation could be modified by this formula. The modified thermal conductivity of the film specimen could be obtained from this implicit formula: $\lambda_{modified} = \lambda_{measured}/(1+y)$. Here, $\lambda_{measured}$ is the measured thermal conductivity based on the original theory. The deviation after modification is within ±6% and much better than original ones.

5. Conclusions

In this work, the thermal conductivity measurement accuracy of thin film specimens using TPS method is numerically studied, seemingly first in the literature. The major conclusions are summarized as follows:

Non-ideal 1D heat conduction in the sensor is generated because of the non-ideal plane source and it's the reason caused the measurement deviation. This makes it difficult to determine the calculation area and calculation thickness. When taking the practical heating area and thickness excluding the heat element for data reduction, the thermal conductivity will be overestimated. Otherwise, the thermal conductivity of film will be underestimated. The option that taking the total sensor area and the insulation thickness including heat element for data reduction will has much better accuracy.

When taking the same option of calculation area and thickness with the instrument software, the deviation decreases rapidly with the increment of the thermal resistance of test film and could be well fitted with an exponential decay curve. The deviation after modification with the fitted formula is basically within ±6% in the full test range.

This work provides a fundamental basis to the accuracy analysis of film thermal conductivity using transient plane source method. The modification proposed in this paper could ensure a good theoretical accuracy of film thermal conductivity measured by transient plane source method.

Acknowledgements

The authors would like to thank the supports from National Natural Science Foundation of China (Grand number 51136004 and 51276138).

References

[1] N. Zamel, E. Litovsky, S. Shakhshir, X. Li, J. Kleiman, Measurement of in-plane thermal conductivity of carbon paper diffusion media in the temperature range of −20 °C to +120 °C, Appl. Energy 88 (9) (2011) 3042–3050.
[2] N. Zamel, E. Litovsky, X. Li, J. Kleiman, Measurement of the through-plane thermal conductivity of carbon paper diffusion media for the temperature range from −50 to +120 °C, Int. J. Hydrogen Energy 36 (19) (2011) 12618–12625.
[3] G. Karimi, X. Li, P. Teertstra, Measurement of through-plane effective thermal conductivity and contact resistance in PEM fuel cell diffusion media, Electrochim. Acta 55 (5) (2010) 1619–1625.
[4] S.G. Kandlikar, Z. Lu, Thermal management issues in a PEMFC stack – a brief review of current status, Appl. Therm. Eng. 29 (7) (2009) 1276–1280.
[5] L. Chen, Y.L. He, W.Q. Tao, The temperature effect on diffusion processes of water and proton in proton exchange membrane using molecular dynamics simulation, Numer. Heat Transf. 64 (4) (2013) 1–13.
[6] L. Chen, H. Lin, W.Q. Tao, Molecular dynamics simulation of temperature effect on diffusion process of water and proton in proton exchange membrane, J. Xi'an Jiao Tong Univ. 45 (7) (2011) 1–4.
[7] L. Chen, W.Q. Tao, Study on diffusion processes of water and proton in PEM using molecular dynamics simulation, in: Materials Science Forum, Trans Tech Publications, 2012, pp. 1266–1272.
[8] H.C. Chien, C.R. Yang, L.L. Liao, C.K. Liu, M.J. Dai, R.M. Tain, D.J. Yao, Thermal conductivity of thermoelectric thick films prepared by electrodeposition, Appl. Therm. Eng. 51 (2013) 75–83.
[9] J.S. Zhang, J.Y. Yang, W. Zhu, C.J. Xiao, H. Zhang, J.Y. Peng, Research advances in the measurement for the thermal conductivity of thin solid films, Mater. Rev. 24 (2010) 103–107.

[10] W.W. Wang, Z. Min, L.Z. Li, Q.J. Liu, Measurement methods and technology of thin-film thermal conductivity, J. Funct. Mater. 41 (2010) 870–873.
[11] A. Cai, L.P. Yang, J.P. Chen, T.G. Xi, S.G. Xin, W. Wu, Thermal conductivity of anodic alumina film at (220 to 480) K by laser flash technique, J. Chem. Eng. Data 55 (2010) 4840–4843.
[12] M. Shamsa, S. Ghosh, I. Calizo, V. Ralchenko, A. Popovich, A.A. Balandin, Thermal conductivity of nitrogenated ultrananocrystalline diamond films on silicon, J. Appl. Phys. 103 (2008) 083538.
[13] ISO22007-2, Plastics—Determination of Thermal Conductivity and Thermal Diffusivity—Part 2: Transient Plane Heat Source (Hot Disc) Method, 2008, pp. 1–16.
[14] D. Chu, M. Touzelbaev, K.E. Goodson, S. Babin, R.F. Pease, Thermal conductivity measurements of thin-film resist, J. Vac. Sci. Technol. B Microelectron. Nanometer Struct. 19 (2001) 2874–2877.
[15] T. Borca-Tasciuc, A.R. Kumar, G. Chen, Data reduction in 3ω method for thin-film thermal conductivity determination, Rev. Sci. Instrum. 72 (2001) 2139–2147.
[16] J.S. Gustavsson, M. Gustavsson, S.E. Gustafsson, On the use of the hot disk thermal constants analyser for measuring the thermal conductivity of thin samples of electrically insulating materials, Therm. Conduct. 24 (24) (1999) 116–122.
[17] M. Gustavsson, E. Karawacki, S.E. Gustafsson, Thermal conductivity, thermal diffusivity, and specific heat of thin samples from transient measurements with hot disk sensors, Rev. Sci. Instrum. 65 (1994) 3856–3859.
[18] K.E. Goodson, M.I. Flik, Solid layer thermal-conductivity measurement techniques, Appl. Mech. Rev. 47 (1994) 101–112.
[19] R. Coquard, E. Coment, G. Flasquin, D. Baillis, Analysis of the hot-disk technique applied to low-density insulating materials, Int. J. Therm. Sci. 65 (2013) 242–253.
[20] S.A. Al-Ajlan, Measurements of thermal properties of insulation materials by using transient plane source technique, Appl. Therm. Eng. 26 (17) (2006) 2184–2191.
[21] V. Goyal, D. Teweldebrhan, A.A. Balandin, Mechanically-exfoliated stacks of thin films of BiTe topological insulators with enhanced thermoelectric performance, Appl. Phys. Lett. 97 (2010) 133117.
[22] S. Malinarič, Uncertainty analysis of thermophysical property measurements of solids using dynamic methods, Int. J. Thermophys. 28 (2007) 20–32.
[23] B.M. Suleiman, Alternative fitting procedures to enhance the performance of resistive sensors for thermal transient measurements, Sens. Actuators Phys. 163 (2010) 441–448.
[24] B.M. Suleiman, S.R. Malinarič, Developments in the data evaluation of the EDPS technique to determine thermal properties of solids, WSEAS Trans. Heat Mass Transf. 4 (2007) 99–110.
[25] B.M. Suleiman, S. Malinarič, Transient techniques for measurements of thermal properties of solids: data evaluation within optimized time intervals, WSEAS Trans. Heat Mass Transf. 12 (2006) 801–807.
[26] V. Bohac, M.K. Gustavsson, L. Kubicar, S.E. Gustafsson, Parameter estimations for measurements of thermal transport properties with the hot disk thermal constants analyzer, Rev. Sci. Instrum. 71 (2000) 2452–2455.
[27] H. Zhang, M.J. Li, W.Z. Fang, D. Dan, Z.Y. Li, W.Q. Tao, A numerical study on the thermal conductivity accuracy of thin film specimens using transient plane source method, in: The Asian Symposium on Computational Heat Transfer and Fluid Flow – 2013, Hong Kong, China, 2013.
[28] H. Zhang, Y. Jin, W. Gu, Z.Y. Li, W.Q. Tao, A numerical study on the influence of insulating layer of the hot disk sensor on the thermal conductivity measuring accuracy, Prog. Comput. Fluid Dyn. 13 (2013) 195–205.
[29] H. Zhang, Y. Jin, W. Gu, Z.Y. Li, W.Q. Tao, A numerical study on the influence of insulating layer of the hot disk sensor on the thermal conductivity measuring when using transient plane source method, in: The Asian Symposium on Computational Heat Transfer and Fluid Flow – 2011, Kyoto, Japan, 2011.
[30] S.E. Gustafsson, Transient plane source techniques for thermal conductivity and thermal diffusivity measurements of solid materials, Rev. Sci. Instrum. 62 (1991) 797–804.
[31] Y. He, Rapid thermal conductivity measurement with a hot disk sensor: part 1. Theoretical considerations, Thermochim. Acta 436 (2005) 122–129.
[32] W.Q. Tao, Numerical Heat Transfer, second ed., Xi'an JiaoTong University Press, Xi'an, 2001.